*International Journal of Multidisciplinary and Current Research* ISSN: 2321-3124
Research Article Available at: http://ijmcr.com

# Numerical Study of Surface Plasmon Resonance of Bimetallic Au-Ag Core-Shell Nanorods

**M. Elalami[*], A. Akouibaa[*] M.Benhamou[#], S. El-fassi[*] and A. Derouiche[*]**

[*]Polymer Physics and Critical Phenomena Laboratory. Hassan II University Casablanca, Sciences Faculty Ben M.sik, P.O. Box 7955, Casablanca, Morocco.
[#]ENSAM, Moulay Ismaïl University, Meknès, Morocco

Accepted 05 Dec 2016, Available online 14 Dec 2016, **Vol.4 (Nov/Dec 2016 issue)**

***Abstract***

*Some metal nanoparticles show distinctive surface plasmon resonance (SPR) bands that consist of intense photo-absorption and light scattering. Because of this characteristic, these nanoparticles are suitable probe materials for sensing and imaging of bio-related materials or for selective targeting in photothermal thearapeutics. The SPR bands come from the collective oscillation of free electrons in nanoparticles that are in resonance with the electromagnetic waves. The resonance frequency strongly depends on the shape and morphology of the nanoparticles. Anisotropic metal nanoparticles have been attractive research targets, because they showed multiple SPR bands in the visible and near infrared regions. Gold and silver core/shell nanorods were known to be uniform rod-shaped metallic core coated with another metallic shell, which clearly showed several surface plasmon bands that originated from the transverse and longitudinal SPR oscillations. In this work a model based on the finite element method (FEM) is developed to investigate the optical properties of Au-core/Ag-shell and Ag-core/Au-shell nanorods with different shell thickness and core aspect ratio. The numerical results that we have obtained show that the absorption spectrum of Au-core/Ag-shell nanorods present three resonance peaks respectively in: near-infrared, visible and ultraviolet regions. Whereas for the Ag-core/Au-shell nanorods the absorption spectrum present two resonance peaks, in near-infrared and ultraviolet regions. For the two cases, the position and amplitude of the various resonance peaks are strongly depends on the molar fraction of composition and core aspect ratio.*

***Keywords:*** *Gold-silver core-shell nanorods, optical properties, surface plasmon resonance, finite element method.*

## 1. Introduction

Noble metal nanoparticles exhibit a strong absorption band in the spectrum, which originates from collective oscillation of conduction electrons [1, 2]. This absorption band is known as the localized surface plasmon resonance (LSPR). The frequencies and intensities of LSPR are known to be sensitive to the dielectric properties of the medium, and in particular, to the refractive index of matter close to the particle surface [3–5]. Therefore, LSPR is a label-free technique that can detect these binding events in real time. These properties open the possibility to develop optical nanosensors based on the noble metal nanoparticles or nanostructures, which are named as LSPR sensors [6,7]. More, this has led to interest in their use as selective biomarkers in biodiagnostics or for selective targeting in photothermal thearapeutics [8].

It is well known that the LSPR performance of noble metal nanoparticles is affected not only by the dielectric properties of the surrounding medium but also by the composition, size and shape of the nanoparticles [9,10]. As far as the sensitivity is concerned, spherical nanoparticles exhibit the poorest sensitivity, while anisotropic structures such as nanorods or triangular nanostructures can achieve higher sensitivity [11,12]. Gold nanorods are characterized by two absorption peaks, corresponding to the plasmon mode from the oscillation of the free electrons along the transverse and longitudinal axis of the nanoparticles. With the aspect ratio of the gold nanorods increasing, the longitudinal band red-shifts, and the refractive index sensitivity is increased. Thus, gold nanorods are of great interest for LSPR sensing because their extinction spectra are highly sensitive to the dielectric constant of the surrounding medium [13,14]. Regarding the materials, Ag nanoparticles prove to be more sensitive than Au nanoparticles with similar structures and resonance wavelength [15].

Metal shell formation on nanoparticles can optimize the electronic, catalytic, and optical properties of nanoparticles [16]. Gold and silver are frequently used for shell or core materials,[16,17] because shell formation of

these elements is a useful way to control the spectroscopic properties of nanoparticles. The distinct surface plasmon (SP) bands of gold and silver are dependent on their sizes and shapes and contribute to enhancing the optical properties of nanoparticles [4]. Recently, bimetallic nanoparticles have induced great interest for their ability to tune the LSPR effect. For example, Fritzsche *et al*. [18] investigated theoretically as well as experimentally the properties of Au-Ag core-shell spherical nanoparticles for refractive index sensing in particle solutions. Au-Ag core-shell spherical nanoparticles showed comparable sensitivities than Au nanorods. Fu *et al*. [19] demonstrated a systematic study on Au-Ag core-shell nanorods by controlling the thickness of the silver shell. Experimental results show that the refractive index sensitivity and figure of merit of the core-shell nanorods can be increased with the coating of Ag shells.

There have been several experimental reports on the optical properties of metal nanoparticles, including gold nanospheres [20], nanorods,[21], bimetallic nanoparticles,[22] composite nanoparticles with a core-shell structure,[23] and nanoparticle chains and assemblies [24]. At the same time, well-established theoretical tools based on the Mie theory [25] , the discrete dipole approximation (DDA) [26] method and the finite element method (FEM) [27,28] have been readily exploited for a quantitative study of the nanoparticle optical properties of different size, shape, composition, and aggregation state, etc [4].

Numerical techniques are designed to solve the relevant filed equation in the computational domain, subject to the boundary constraints imposed by the geometry. Without making a priori assumption about which field interaction are most significant, numerical techniques analyze the entire geometry provided as input. The finite element method (FEM) [29], which is a powerful numerical modeling tool, has been widely used for modeling electromagnetic wave interaction with complex materials. Recently, Benhamou *et al*. [30,31] have used this method to study the plasmonic resonance of gold nanoparticles with various sheep and morphology. In this paper, we use the FEM approach for computing the potential distribution in the composite material consisting of the gold-silver core/shell nanorods randomly oriented in a dielectric medium and to derive its effective dielectric constant, this parameter allowed us to calculate the absorption cross-section. The properties of the localized surface plasmon resonance (LSPR) of two core-shell bimetallic nanostructures, that is the monodisperse Au-core/Ag-shell and Ag-core/Au-shell nanorods with different shell molar fraction and aspect ratio of the core, are simulated and discussed. The obtained results show that the position and amplitude of the optical resonance peaks vary depending on the molar, mass and volume fractions of the shell.

## 2. Methodology and Model

### *2.1 Modeling of core-shell bimetallic Nanorods.*

The creation of core/shell nanoparticles (CSNs) has in recent years developed into an increasingly important research area at the frontier of advanced materials chemistry [32,33]. The importance stems largely from the diverse attributes of CSNs as model building blocks towards functional materials. Many types of nanoparticles could fit into the core/shell category, which is recently broadly defined as core and shell of different matters in close interaction, including inorganic/organic, inorganic/inorganic, organic/organic, or inorganic/biological core/shell combinations [34]. In

Particular Gold and silver core-shell nanorods (Au@Ag CSNRs), with their controllable monodispersity and aspect ratio, broad plasmon resonance tunability from near-UV to the IR range, as well as the much sharper and stronger longitudinal SPR bands relative to those of GNRs, have been successfully utilized in areas such as solar energy development [35], near-IR hyperthermia and nonlinear optical imaging [36]. Even so, little has been reported on their application to immunoassay [37].

In the present work, the objective is to study the optical properties of Au@Ag bimetallic core/shell nanorods using the finite element method. In order to implement the finite elements scheme we have modeled these nanoparticles with a core/shell uniform structure consisting of two coaxial cylinders one is at the inner on the other, the inner cylinder represents the nanoparticle core and that of the outer represents the shell. The fitting geometrical parameters for this structure model are: the aspect ratio of the core that is defined by the quotient $\eta_c = {}^{h}/_{2r}$ such as that $h$ is the nanorod height and $r$ its radius, the shell thickness is denoted $e$. The aspect ratio of the Au@Ag core/shell nanoparticle is $\eta_c = {}^{H}/_{2R}$ such as $H$ is the total height of the nanoparticle and $R$ its radius which are given by $H = h + 2e$ and $R = r + e$. This nanoparticle is considered immersed in a dielectric medium as shown in Fig.1.

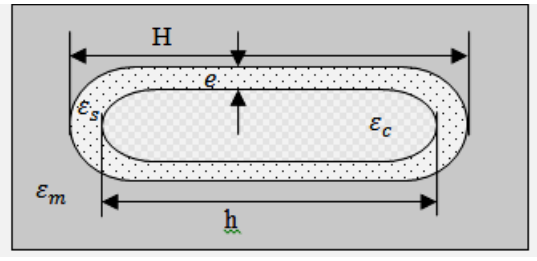


**Fig.1** Representation of the core-shell nanorod model

The physical parameter characterizing the different phases of this nanocomposite structure is the dielectric permittivity of each component which is denoted as follows: $\varepsilon_c$ for the metallic core, $\varepsilon_s$ for the metallic shell and $\varepsilon_m$ for the surrounding medium. The dielectric constant of gold and silver is a function of electromagnetic wave frequency with which it interacts.

Indeed, the interaction of the electromagnetic wave defined by its pulsation $\omega$, with a metal lead to polarization of the medium. This polarization then generates a change in the complex refractive index, $\tilde{n}(\omega)$ which is related to the dielectric constant by the following relationship: $\tilde{n}^2(\omega) = \varepsilon(\omega)$.

*2.2 Dielectric Permittivity of Noble Metal*

The frequency-dependent electric permittivity is an important parameter to be known in advance when studying the frequency response of the material over a wide frequency range. Traditionally, Drude-Lorentz (DL) model which can well represent the optical properties of the metal originating from the interband and intraband transitions was the popular one and has been used to quantify the dispersion properties of the metal [38-40]. In DL model, a large number of Lorentz oscillators can be used to model the line shape of the electric permittivity of the material over the frequency range of interest [40]. However, the accuracy improvement obtained via adding more Lorentz terms comes with a price. A large number of Lorentz terms lead to increased requirement of computational resources such as CPU power and memory [41].

Recently, Drude-critical point (DCP) model that consists of one Drude term and two or three critical points terms denoted respectively Two-DCP and Three-DCP models was proposed which can satisfactorily represent the electric permittivity of noble metals over a wide frequency range [42]. From the computational perspective, Two-DCP and Three-DCP models are advantageous over DL model since the former requires only less number of terms. Since then, Two-DCP and Three-DCP models have been used to represent the electric permittivity of noble metals such as gold and silver with good accuracy [43].

The DCP dispersive model expresses interband transitions featuring asymmetric line shapes with critical point terms instead of Lorentzian terms [40]. The relative dielectric permittivity of gold as per the Two-DCP model can be written as:

$$\varepsilon_{Au}(\omega) = \varepsilon_\infty + \chi_D(\omega) + \sum_{p=1}^{2} \chi_p(\omega) \quad (1)$$

Where $\varepsilon_\infty$ is the relative electric permittivity at infinite frequency, $\chi_D(\omega)$ the Drude susceptibility, and $\chi_p(\omega)$ the critical point susceptibility. The Drude susceptibility is expressed as:

$$\chi_p(\omega) = -\frac{\omega_D^2}{\omega^2 + i\gamma\omega} \quad (2)$$

Where $\omega_D$ is the Drude pole frequency and $\gamma$ the inverse of the pole relaxation time. Also, the critical point susceptibility is expressed as:

$$\chi_p(\omega) = A_p\Omega_p\left(\frac{e^{i\phi_p}}{\Omega_p - \omega - i\Gamma_p} + \frac{e^{-i\phi_p}}{\Omega_p + \omega + i\Gamma_p}\right) \quad (3)$$

Where $A_p$ is the amplitude, $\phi_p$ the phase, $\hbar\Omega_p$ the energy gap, and $\Gamma_p$ the broadening of the pole.

A final model is the three-critical points Drude model (three-CPDM) [44] that also describes the dielectric function of silver. We recall that the use of three-CPDM, for the description of the permittivity of silver in a wide frequency band, makes sense only when the frequency-band is in the interval $0.6\text{eV}$ to $6.87\text{eV}$, corresponding to wavelengths between $181\text{nm}$ and $2069\text{nm}$. We note that this model is more accurate than the four points Lorentz one that is described in literature [45]. In this model, the permittivity expression of silver nanoparticles is

$$\varepsilon_{Ag}(\omega) = \varepsilon_\infty + \frac{\sigma}{i\varepsilon_0\omega} + \sum_{p=1}^{3} \chi_p(\omega) \quad (4)$$

*2.3 Numerical Method*

In this work we are interested in determining the effective dielectric permittivity of nanocomposite constituted by gold-silver core/shell nanorods immersed in a dielectric medium using the Finite Element FE numerical tool. The detailed description of the method for determining the effective permittivity in the quasi-static limit can be found elsewhere [46]. As both computing power and the efficiency of the FE computational method, it is becoming possible to investigate new composite materials through computer simulations before they have even been synthesized. FE tool is used to compute the solution of Laplace equation by determining the electric field and potential distribution from the physical properties of different phases of the composite material. Recent works have shown that the FE method could be successfully applied to compute the effective permittivity of periodic composite materials [47]. The basic scheme of the FE method is now briefly recalled.

To describe the FEM scheme, we consider a spatial domain $\Omega$ contains Au-Ag core/shell nanorod shown in Fig.2 with a vanishing charge density. Solving the problem at hand means finding the local potential distribution inside the computational domain by solving Laplace's equation (first principal of electrostatic):

$$\vec{\nabla}\left(\varepsilon_0\varepsilon(\vec{r})\vec{\nabla}V(\vec{r})\right) = 0\,, \quad (5)$$

Where $\varepsilon(r)$ and $V(\vec{r})$ are the local relative permittivity and the potential distribution inside the material domain respectively with zero charge density.$\varepsilon_0 = 8.85.10^{-12}\,\text{F/m}$ is the permittivity of the vacuum. In addition, the composite (dielectric) is assumed to be periodic with three phases (metallic core, metallic shell and host matrix). Taking into account the symmetry and periodicity properties, the geometry of the medium is reduced to a unit cell. The implementation of the FE method consists in dividing the three-dimensional domain into tetrahedral finite elements and interpolating the potential $V$ and its normal derivative $\frac{\partial V}{\partial n}$ on each finite

element similarly to the BIE method [48] with the corresponding nodal values:

$$V = \sum_i \lambda_i V_i \quad (6)$$

$$\frac{\partial V}{\partial n} = \sum_i \lambda_i \left(\frac{\partial V_i}{\partial n}\right) \quad (7)$$

Where $\lambda_i$ denotes the interpolating functions.

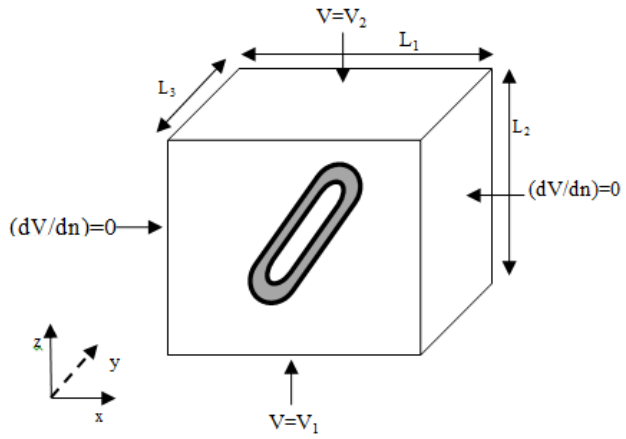


**Fig. 2** Notation and boundary conditions related to three dimensional periodic nanocomposite

Following this analysis, the solution of Laplace's equation is obtained using the Galerkin method and by solving the resulting matrix equation from the boundary conditions thanks to a standard numerical technique, i.e., Gauss procedure [31].

Having computed the potential and its normal derivative on each tetrahedron of the computational mesh, the electrostatic energy $W_e^k$, and losses, $P_e^k$ could be expressed for each tetrahedral element as:

$$W_e^k = \frac{\varepsilon_0}{2} \iiint_{V_k} \varepsilon_k'(x,y,z) \left[\left(\frac{\partial V}{\partial x}\right)^2 + \left(\frac{\partial V}{\partial y}\right)^2 + \left(\frac{\partial V}{\partial z}\right)^2\right] dV_k \quad (8)$$

$$P_e^k = \frac{\varepsilon_0}{2} \iiint_{V_k} \omega\varepsilon_k''(x,y,z) \left[\left(\frac{\partial V}{\partial x}\right)^2 + \left(\frac{\partial V}{\partial y}\right)^2 + \left(\frac{\partial V}{\partial z}\right)^2\right] dV_k \quad (9)$$

Where $\varepsilon_k$ and $V_k$ represent the permittivity and the volume of the $k^{th}$ tetrahedron element, respectively. Thus, the total energy and losses in the entire composite can be written by summation over the $n_k$ elements such as:

$$W_e = \sum_{k=1}^{n_k} W_e^k \quad (10)$$

$$P_e = \sum_{k=1}^{n_k} P_e^k \quad (11)$$

To compute quantities $W_e$ and $P_e$, we suppose that the composite material is embedded in a plane capacitor. This way allows us to determine the effective permittivity in a direction parallel to the applied electric field. Then, from the capacitor electrostatic energy expression, we deduce the effective (complex) permittivity. We find that the real part, $\varepsilon_{eff}'$, and imaginary one, $\varepsilon_{eff}''$, parallel to the applied electric field, are given by:

$$W_e = \frac{1}{2}\varepsilon_{eff}' \frac{S_d}{L_3}(V_2 - V_1)^2, \quad (12)$$

$$P_e = \frac{1}{2}\omega\varepsilon_{eff}'' \frac{S_d}{L_3}(V_2 - V_1)^2. \quad (13)$$

Where $V_1$ and $V_2$ are the potentials applied across to plates of the unit cell (Fig. 2). Here, $S_d = L_1.L_3$ is the surface of in-depth. The real and imaginary parts of the effective permittivity then depends on the total energy, $W_e$, losses, $P_e$, linear size $L_2$ and applied potential difference $V_2 - V_1$. In addition, the second one is frequency-dependent. If the amplitude of the applied field is equal to 1, so the potential difference is kept equal to $\Delta V = L_2$. The following paragraph will be devoted to the determination of the optical properties of the material under investigation.

### *2.4 Absorption-cross-section*

From the evolution of the effective complex dielectric function depending on the wavelength (or frequency) of the incident field, the resonance modes that may occur in nanoparticles are identified. For this, it would be interesting to calculate the scattering cross-sections and absorption. The sum of these two quantities defines the extinction cross-section.

$$\sigma_{ext} = \sigma_{abs} + \sigma_{diff}. \quad (14)$$

In the case where the dimensions are very small compared to the wavelength, the light scattering can be ignored, and we have: $\sigma_{ext} \approx \sigma_{abs}$

The cross-section of extinction (absorption) can be determined from the imaginary part of the effective dielectric function of the composite using the following equation [49].

$$\sigma_{abs} = \frac{V_p}{f}\frac{k}{n_{eff}}\varepsilon_{eff}'' \quad (15)$$

Here, $V_p$ stands for the common volume of nanoparticles, f is their fraction, k is the wave-vector amplitude of the electromagnetic wave, and $n_{eff}$ represents the refractive index that can be related to the real and imaginary parts, $\varepsilon_{eff}'$ and $\varepsilon_{eff}''$, of the effective permittivity by [50].

$$n_{eff} = \left(\frac{\sqrt{\varepsilon_{eff}'^2 + \varepsilon_{eff}''^2} + \varepsilon_{eff}'}{2}\right)^{1/2} \quad (16)$$

This formula clearly shows that the peak of $\mathrm{Im}(\varepsilon_{eff})$ indicates that the light is rather absorbed in specific regions. The effective dielectric function and the effective refraction index are calculated using FEM. Hence, the section of optical absorption is easily obtained. In the following section, we present and discuss our findings.

## 3. Results and discussion

Gold nanorods, owing to their attractive advantages, including facile growth methods, tunable longitudinal

plasmon wavelengths, and chemical stability, can function as excellent supports for the formation of Ag shells. The resultant Au-core/Ag-shell nanorods are expected to exhibit plasmonic properties that are determined by silver. At the same time, the plasmon wavelengths of the core-shell nanorods can be tailored in the visible to near-infrared spectral regions by varying the Au core size and the Ag shell thickness. On the basis of this reasoning, Au-core/Ag-shell nanostructures in different shapes, including dumbbells, rods, and octahedrons, have been prepared by different methods. Upon Ag coating, the lowest-energy plasmon band is generally blue-shifted and new plasmon bands are generated simultaneously at higher energies. The lowest-energy plasmon band is usually attributed to the longitudinal mode. The number of the newly generated plasmon bands is dependent on the shape of the core/shell nanostructures. However, the exact nature of the newly generated plasmon bands has not been investigated systematically and still remains controversial. Unraveling the nature of these plasmon bands is of vital importance because different plasmon modes exhibit distinct optical properties. For example, dipolar plasmon modes can radiate efficiently to the far field while quadrupolaire plasmon modes only take effect in the near-field region mostly. In this work we are interested in the study of the optical properties of two core/shell nanostructures using the FEM, The first structure is a gold-core/silver-shell nanorod and the second is a silver-core/gold-shell nanorod. Due to the anisotropy of structure the core/shell bimetallic nanorods exhibit transverse (T) and longitudinal (L) plasmon resonance modes that correspond to the electron oscillations which are perpendicular and parallel to the length axis of the nanorod, respectively. When the inclusions are dispersed in a dielectric medium with arbitrary orientations that lead to the appearance of multiple resonances modes, in the same absorption spectrum, who corresponds to the longitudinal mode (L-mode), transversal (T-mode) and dipolar or quadrupolaire interactions. Two important approaches that intervene in implementation of FEM that we have used in this work: the first is the quasi-static approximation, for which the inclusions have small sizes compared to incident electromagnetic wavelength, that's the reason to can consider uniform electric field in the particle. The second is the volume fraction $\phi_v$ of inclusion relative to the surrounding medium that must be very small to can neglect the interparticle coupling effect.

Consider a nanorod consists of a gold core coated with a silver shell with the following geometrical parameters: height and radius of gold core respectively h = 40 nmand r=5nm, aspect ratio of core η =h⁄2r=4 and silver shell thickness is denoted e.This core/shell nanorod is randomly immersed in an aqueous dielectric medium of its permittivity $\varepsilon_m = 1.77$ with volume fraction $\phi_v = 0.05$. In a first stage we will study the effect of the composition of this nanocomposite on their optical properties via the surface plasmon resonance (SPR) absorption peak. Fig.3 shows the variation of the absorption cross section for different values of the silver shell thickness. For pure gold nanorods, there are two SPR absorption peaks corresponding to transverse and longitudinal resonance appearing at about 508.8 and 743.4 nm, respectively. As the coating Ag shell thickness is increased from 1 to 4 nm, both the longitudinal (denoted as peak 1) and transverse (denoted as peak 2) peaks blue shift and get intense. However, the shifting and intensity increase of the longitudinal peak are more intense. What is more, the Ag coating results in a new plasmonic absorption peak taking place at shorter wavelength, which is denoted as peak 3. As the coating Ag shell thickness is increased, the peak 1 red shifts slightly and gets intense greatly. All these Ag coating-dependent absorption properties are in good agreement with the experimental results [51]. Because the Ag nanoparticles have more intense plasmonic absorption, the physical mechanism of the intensity increasing of peaks 1 and 2 could be resulted from the increase composition of Ag in the Au–Ag bimetallic nanoparticles [51]. Because the Ag nanoparticles have shorter plasmon resonance wavelength, the intense blue shift of peaks 2 and 3 should also be attributed to the increase composition of Ag in the bimetallic nanoparticles. On the other hand, a homogeneous Ag layer coating lowers the overall aspect ratio of the core–shell nanostructure which provides the minor reason of the blue shift of peak 1.

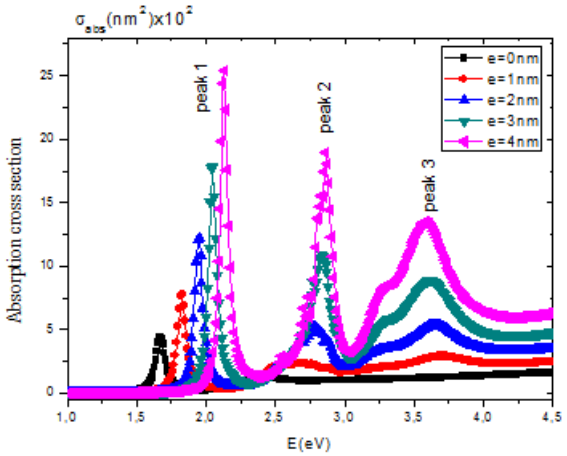


**Fig.3** Evolution of the absorption cross section of gold-core/silver-shell nanorod upon photon energy for different values of silver-shell thicknesses

The composition of the Au-core/Ag-shell nanorods can be determined by the molar fraction of the silver shell noted $\phi_s$. Fig.4 depicts the dependences of the plasmon peak wavelengths $\lambda_{max}$ on the Ag-shell molar fraction. Because the Ag shell thickness is controlled by the amount of Ag used during the synthesis, the amount of Ag corresponds to the Ag shell thickness, and the Ag shell thickness is increased as the amount of Ag is increased. The curves show that increasing the silver coating results in linearly shifting of three resonance peaks, towards blue wavelengths for the peaks 1 and 2, and red shifting for

the peak 3. These numerical results are in good agreement with experimental observations found by Jian Zhu *et al* [52].

Another parameter which plays a crucial role in determining the optical properties of metallic nanorods is the aspect ratio, denoted $\eta$ this parameter determines the nanoparticle geometry is defined as the ratio of the nanorod height on their diameter $\eta = {}^{h}/_{2r}$ with r is the nanorod radius. Several experimental and theoretical studies have been conducted on the effect of the aspect ratio on the spectral properties of the isolated gold nanorods with and without coating [21,53-55]. These studies showed that the wavelength corresponding to the longitudinal plasmon resonance mode varies linearly according the nanorod aspect ratio. Fig.5 shows the variation of the absorption cross section of Au-core /Ag-shell nanorods for various values of gold-core aspect ratio. These curves are obtained when fixing the silver-shell thickness at $e = 3nm$, volume fraction $\phi_v = 0.05$ and surrounding medium dielectric permittivity $\varepsilon_m = 1.77$. These curves show that, when the gold-core aspect ratio varies from $\eta = 3$ to $\eta = 5$, the position of the three resonance peaks are shifted as follows: peak1 red shifting (from $580.15nm$ to $633.22nm$), peak2 slightly blue shifting (from $456.44nm$ to $437.16nm$) and the third peak3 very slightly red shifting (from $342nm$ to $345$ nm). These shifts are accompanied by an increase in absorption intensity for the peak 1 and a decrease in intensity for the peaks2 and 3. The dependence of the wavelength $\lambda_{max}$ corresponding to the SPR of the three peaks to the gold-core aspect ratio $\eta$ is represented in Fig.6 that shows the linear variation of $\lambda_{max}$ depending to $\eta$.

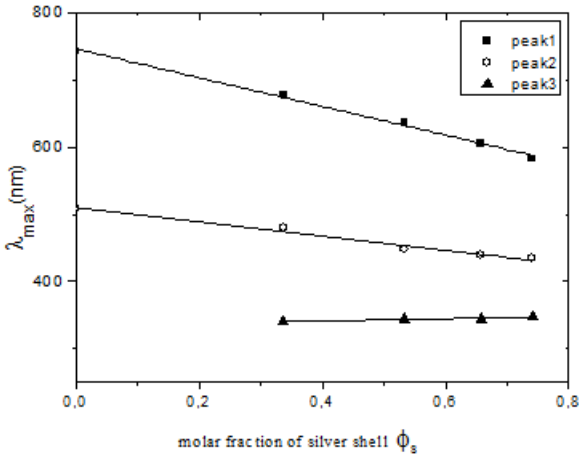


**Fig.4** Evolution of the $SPR - \lambda_{max}$ position for the three resonance peaks upon molar fraction of silver-shell of gold-core/silver-shell nanorods.

Noble metals and their compounds have a long and distinguished history as therapeutic agents in medicine. Recent years have seen tremendous progress in the design and study of nanomaterials geared towards biological and biomedical applications. Particularly gold nanoparticles have attracted intensive interest, because they are easily prepared, can be readily attached to molecules of biological interest and did not show any indication of toxicity contrary to silver nanoparticles [56]. Because of the non-toxicity of gold bimetallic gold-silver core/shell nanoparticles whose shell is the gold are considerable interest. In this section we will study the optical properties of silver-core/gold-shell nanorods. For this Consider a nanorod consists of a silver core coated with a gold shell with the following geometrical parameters: height and radius of silver core respectively $h = 40$ nm and $r = 5nm$, aspect ratio of core $\eta = 4$ and gold shell thickness is denoted e. This core/shell nanorod is randomly immersed in an aqueous dielectric medium of its permittivity $\varepsilon_m = 1.77$ with volume fraction $\phi_v = 0.05$. The optical properties of this nanocomposite are investigated using the EMF. Fig.7 shows the variation of the absorption cross section in function of the photon energy, for different values of the gold-shell thickness.

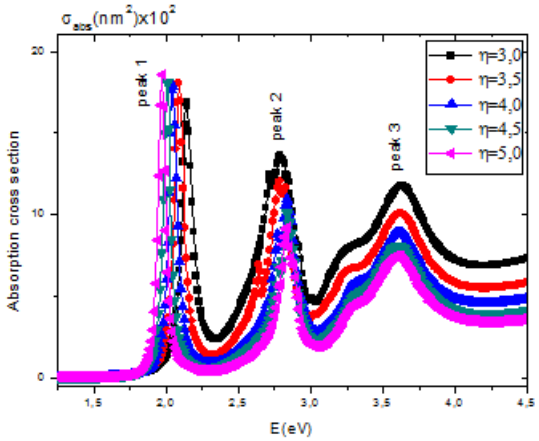


**Fig.5** Evolution of the absorption cross section of gold-core/silver-shell nanorod upon photon energy for different values of gold-core aspect ratio

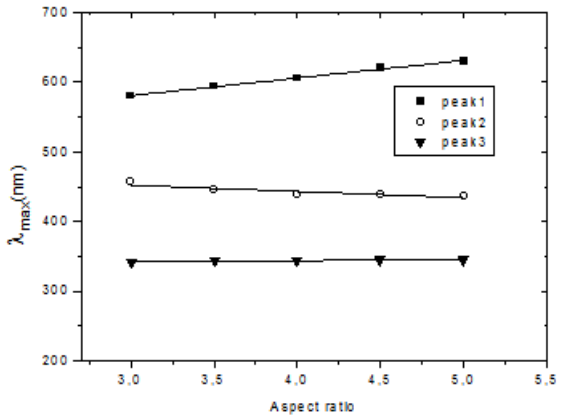


**Fig.6** Evolution of the $SPR - \lambda_{max}$ position for the three resonance peaks upon gold-core aspect ratio of gold-core/silver-shell nanorods

These curves show that when the gold-shell thickness varies from $e = 1nm$ to $e = 4nm$, the SPR peak position shift toward the blue wavelength from $\lambda_{max} = 646.63nm$

to $\lambda_{max} = 630.22nm$, this shifting is accompanied by a slight increase in amplitude of absorption. Fig.8 shows the variation of wavelength $\lambda_{max}$ corresponding to the SPR depending on the gold-shell molar fraction. This figure shows that the $\lambda_{max}$ position decreases linearly in function of the gold-shell mole fraction.

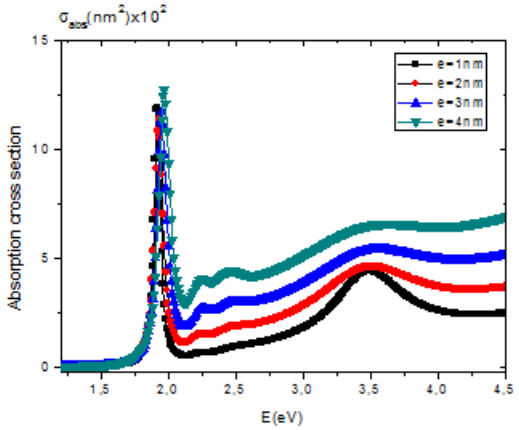


**Fig.7** Evolution of the absorption cross section of silver-core/gold-shell nanorod upon photon energy for different values of gold-shell thicknesses

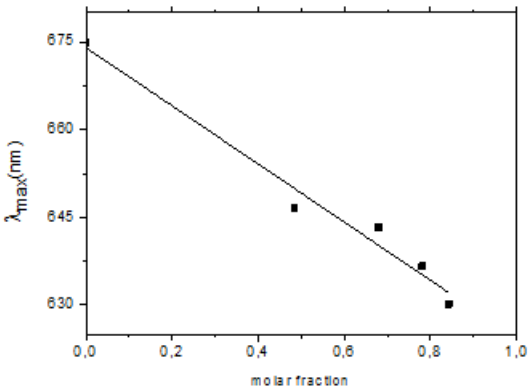


**Fig.8** Evolution of the $SPR - \lambda_{max}$ position for the resonance peak upon molar fraction of gold-shell of silver-core/gold-shell nanorods

## Conclusions

We recall that the present work deals with the study of the optical properties of (Au-Ag) bimetallic core-shell nanorods. The investigation of these of nanomaterials can be justified by their potential applications in various fields including sensing, biological imaging, optical and optoelectronic devices and cancer therapy. Another advantage is that, these nanostructures give rise to multiple SPR peaks, and then promise new potential applications. We have established a series of 3D-simulations using FEM to determining the optical properties of bimetallic core/shelled nanorods with multiple phases, which are embedded in a host dielectric medium. More precisely, we have computed the effective permittivity of these nanostructures, upon compositions and natures of cores and shells metal. In particular, the study revealed that the absorption spectrum of gold-core/silver-shell nanorod presents three resonances peaks corresponding to different transverse and longitudinal modes. The obtained results show that increasing the silver coating results in linearly shifting of three resonance peaks, towards blue wavelengths for the peaks 1 and 2, and red shifting for the peak 3. These numerical results are in good agreement with experimental observations found by Jian Zhu *et al* [55].

The second system that we have studied in this work is the silver-core/gold-shell nanorod. The advantage of the latter due to the non toxicity of gold which will be at the external layer of the nanoparticle which provides the possibility to use these nanoparticles in therapy with more confidence. The obtained results show that when the gold coating increases the SPR peak position shift toward the blue wavelength, this shifting is accompanied by a slight in amplitude of absorption. As pointed out before, the simulation results presented in this paper were found to be in good agreement with very recent experiment. Then, FEM approach provides a powerful tool for the study of the optical properties of nanoparticles with different compositions and shapes.

Finally, we emphasize that the numerical method developed in this work, for the investigation of the optical properties of clothed nanoalloys, can be extended to other types of metal nanoparticles, of different sizes and shapes, as nanoshells, nanocages and nanotips, in order to improve the optical properties suitable for biomedical applications. In addition, we emphasize that the developed numerical method can be extended to investigate the electromagnetic coupling between particles and its effect on the plasmonic behaviors. Such considerations are in progress.

## References

[1]. A.J. Haes and R.P. Van Duyne (2004) A unified view of propagating and localized surface plasmon resonance biosensors, *Anal Bioanal Chem.,* 379, pp.920–930.

[2]. H.J. Chen, T. Ming, L. Zhao, F. Wang, L.D. Sun, J.F. Wang and C. H. Yan (2010) Plasmon molecule interactions, *Nano Today*, 5, pp.494–505.

[3]. M.D. Malinsky, K. Lance Kelly, G.C. Schatz and R.P. Van Duyne (2001) Chain length dependence and sensing capabilities of the localized surface plasmon resonance of silver nanoparticles chemically modified with alkanethiol self-assembled monolayers, *J Am Chem Soc.,* 123, pp.1471–1482.

[4]. K. Lance Kelly, E. Coronado, L.L. Zhao and G.C. Schatz (2003) The optical properties of metal nanoparticles: the influence of size, shape, and dielectric environment. *J Phys Chem B*, 107, pp.668–677.

[5]. M.D. Malinsky, K. Lance Kelly, G.C. Schatz and R.P. Van Duyne (2001) Nanosphere lithography: effect of substrate on the localized surface plasmon resonance spectrum of silver nanoparticles, *J Phys Chem B*, 105, pp.2343–2350.

[6]. M. Amjadi and E Rahimpour (2012) Silver nanoparticles plasmon resonance-based method for the determination of

uric acid in human plasma and urine samples, *Microchim Acta*, 178, pp.373–379.

[7]. B. Sepúlvedaa, P.C. Angeloméb, L.M. Lechugaa and L.M. Liz-Marzánb (2009) LSPR-based nanobiosensors, *Nano Today*, 4, pp.244–251.

[8]. N.R.JANA, L.A. GEARHEART and C.J. MURPHY (2001) Seed-mediated growth approach for shape-controlled synthesis of spheroidal and rod-like gold nanoparticles using a surfactant template, *Advanced Materials* 13, pp.1389-1393.

[9]. K.M. Mayer and J.H. Hafner (2011) Localized surface plasmon resonance sensors, *Chem Rev*, 111, pp.3828–3857.

[10]. M.B. Cortie and A.M. McDonagh (2011) Synthesis and optical properties of hybrid and alloy plasmonic nanoparticles, *Chem Rev*, 111, pp.3713–3735.

[11]. H.J. Chen, X.S. Kou, Z. Yang, H. NiW and J.F. Wang (2008) Shape- and sizedependent refractive index sensitivity of gold nanoparticles, *Langmuir*, 24, pp.5233–5237.

[12]. Y.G. Sun and Y.N. Xia (2002) Increased sensitivity of surface plasmon resonance of gold nanoshells compared to that of gold solid colloids in response to environmental changes, *Anal Chem*, 74, pp.5297–5305.

[13]. S.M. Marinakos, S.H. Chen, A. Chilkoti (2007) Plasmonic detection of a model analyte in serum by a gold nanorod sensor, *Anal Chem*, 79, pp.5278–5283.

[14]. X. Xu, Y.B. Ying and Y.B. Li (2011) Gold nanorods based LSPR biosensor for label-free detection of alpha-fetoprotein *Procedia Eng.*, 25, pp.67–70.

[15]. Y.H. Lee, H.J. Chen, Q.H. Xu and J.F. Wang (2011) Refractive index sensitivities of noble metal nanocrystals: the effects of multipolar plasmon resonances and the metal type, *J Phys Chem C*, 115, pp.7997–8004.

[16]. S. Kalele, S. W. Gosavi, J. Urban and S. K. Kulkarini (2006) Nanoshell particles: synthesis, properties and applications, *Curr. Sci.*, 91, pp.1038–1052.

[17]. C. Wang, S. Peng, R. Chan and S. Sun (2009) Synthesis of Au-Ag Alloy Nanoparticles from Core/Shell Structured Ag/Au, *Small*,5, pp.567–570.

[18]. A. Steinbrück, O. Stranik, A. Csaki, W. Fritzsche (2011) Sensoric potential of gold–silver core–shell nanoparticles, *Anal Bioanal Chem,* 401, pp.1241–1249.

[19]. Q. Fu, D.G. Zhang, M.F. Yi, X.X. Wang, Y.K. Chen, P. Wang and H. Ming (2012) Effect of shell thickness on a Au-Ag core-shell nanorodsbased plasmonic nano-sensor, *J. Opt*., 14, pp.085001–085006.

[20]. S. Link and M.A. El-Sayed, (1999) Spectral Properties and Relaxation Dynamics of Surface Plasmon Electronic Oscillations in Gold and Silver Nanodots and Nanorods, *J. Phys. Chem. B*, 103, pp.8410-8426.

[21]. C.F. Bohren and D.R. Huffman, Absorption and Scattering of Light by Small Particles; John-Wiley: *New York*, (1983).

[22]. C. Sonnichsen, T. Franzl, T. Wilk, G. von Plessen, J. Feldmann, O. Wilson and P. Mulvaney, (2002) Drastic Reduction of Plasmon Damping in Gold Nanorods, *Phys. ReV. Lett.*, 88, pp.77402(1-4).

[23]. F. Hubenthal, T. Ziegler, C. Hendrich, M.Alschinger and F. Trager, (2005) Tuning the surface plasmon resonance by preparation of gold-core/silver-shell and alloy nanoparticles, *Eur. Phys. J. D*, 34, pp.165-168.

[24]. S.J. Oldenburg, R.D. Averitt, S.L. Westcott, N.J. Halas, (1998) Nanoengineering of optical resonances, *Chem. Phys. Lett.*, 288, pp.243-247.

[25]. N. Félidj et al, (2004) Gold particle interaction in regular arrays probed by surface enhanced Raman scattering, *J. Chem. Phys.*, 120, 7141-7146.

[26]. G. Mie, (1908) contributions to the optics of diffuse media, especially colloid metal solutions, *Ann. Phys. (Leipzig)*, 25, pp.377-445.

[27]. B.T. Draine and P.J.J. Flatau, (1994) Discrete-dipole approximation for periodic targets: theory and tests, *Opt. Soc. Am. A*, 11, pp.1491-1499.

[28]. A. Akouibaa, M. Benhamou et al, (2012) numerical study of the plasmonic resonance of multi-phases nanoparticles, *Inter. Jou. Aca. Res.*, 4. No. 6, pp. 213-223.

[29]. J.N. Reddy, An Introduction to Finite Element Method, 2nd., Mc Graw Hill, *New York*, (1993); See also O.C. Zienkiewicz and R.L. Taylor, The Finite Element Method, Vol. 1, McGraw-Hill, *London*, (1989).

[30]. M. Benhamou, A.R. Senoudi, F. Lallam, A. Boussaid and A. Bensafi, (2010) Optical Properties Of Anisotropic Nanogolds From Finite Element Method, *Science & Nano Technology: An Indian Journal*, vol.4.

[31]. A.Akouibaa, M. Benhamou, A. Derouiche, (2013) Simulation of the Optical Properties of Gold Nanorods: Comparison to Experiment, *IJARCSSE*, 3(9), pp.657-671.

[32]. A.C. Templeton, W.P. Wuel.ng and R.W. Murray, (2000) Monolayer-protected cluster molecules, *Acc. Chem. Res.*, 33, pp.27-36.

[33]. F. Caruso, (2001) Nanoengineering of Particle Surfaces, *Adv. Mater*, 13, pp.1-11.

[34]. C.A. Mirkin, R.L. Letsinger, R.C. Mucic and J.J. Storhoff, (1996) A DNA-based method for rationally assembling nanoparticles into macroscopic materials, *Nature*, 382, pp.607-613.

[35]. Y.Q.Qu, R. Cheng, Q.Su and X.F.Duan, (2011), Plasmonic Enhancements of Photocatalytic Activity of Pt/n-Si/Ag Photodiodes Using Au/Ag Core/Shell Nanorods, *Journal of the American Chemical Society* 133 (42), pp.16730–16733.

[36]. K.W.Hu, T.M.Liu, K.Y.Chung, K.S.Huang, C.T. Hsieh, C.K. Sun and C.S. Yeh, (2009) Efficient near-IR hyperthermia and intense nonlinear optical imaging contrast on the gold nanorod-in-shell nanostructures, *Journal of the American Chemical Society*, 131 (40), pp.14186-14187.

[37]. Z.Y. Wang, S.F.Zong, W. Li, C.L.Wang, S.H.Xu, H.Chen and Y.P.Cui, (2012) SERS-Fluorescence Joint Spectral Encoding Using Organic-Metal-QD Hybrid Nanoparticles with a Huge Encoding Capacity for High-Throughput Biodetection: Putting Theory into Practice, *Journal of the American Chemical Society*, 134 (6),pp. 2993–3000.

[38]. K.H. Lee et al, (2011) Implementation of the FDTD method based on lorentz-drude dispersive model on GPU for plasmonics applications, *Prog. In Elect. Res.*, 116, pp.441-456.

[39]. A. Shahmansouri, and B. Rashidian, (2012) GPU Implementation of Split-Field Finite-Difference Time-Domail Method for Drude-Lorentz Dispersive Media, *Prog. In Elect. Res.*, 125, pp.55-77.

[40]. P. G. Etchegoin, E. C. Le Ru, and M. Meyer, (2006) An analytic model for the optical properties of gold, *J. Chem. Phys.*, 125 No. 16, pp.164705-164708.

[41]. J.L. Young, and R.O. Nelson, (2001) A summary and systematic analysis of FDTD algorithms for linearly dispersive media, *IEEE Antennas Propag. Mag.*, 43 No. 1, pp.61-77.

[42]. P. G. Etchegoin, , E. C. Le Ru, and M. Meyer, (2007) Erratum: An analytic model for the optical properties of gold, *J. Chem. Phys.*, 127 No. 18 , pp.189901.

[43]. A. Vial, and T. Laroche, (2008) Comparison of gold and silver dispersion laws suitable for FDTD simulations, *Appl. Phys. B*, 93, No. 1, pp.139-143.

[44]. Lu, J. Y., and Y. H. Chang. "Implementation of an efficient dielectric function into the finite difference time domain method for simulating the coupling between localized surface plasmons of nanostructures." *Superlattices and Microstructures* 47.1 (2010): 60-65.

[45]. F. Hao and P.Nordlander, (2007) Efficient dielectric function for FDTD simulation of the optical properties of silver and gold nanoparticles, *Chem. Phys. Letter*. 446 pp.115-118.

[46]. V. Myroshnychenko and C. Brosseau, (2005) Finite-element method for calculation of the effective permittivity of random inhomogeneous media, *Phys. Rev. E*, 7, pp.016701-016716.

[47]. N. Jebbor and S. Bri, (2012) Effective permittivity of periodic materials: Numerical modeling by the finite element method, *J. of Electrostatics*, 70, pp.393-399.

[48]. B. Sareni, L Krähenbühl, A. Beroual, and C. Brosseau, (1996) Effective dielectric constant of periodic composite materials, *J. Appl. Phys.*, 80(3), 1688-1696.

[49]. G. Weick, R.A. Molina, D. Weinmann and R.A. Jalabert, (2005) Life-time of the first and second collective excitations in metallic nanoparticles, *Phys. Rev. B*, 72, pp.115410 (1-17).

[50]. E.D. Palik, Handbook of Optical Constants of Solids III, Academic Press, *New York*, (1991).

[51]. M.Z. Liu, P. Guyot-Sionnest, (2004) Synthesis and optical characterization of Au/Ag core/shell nanorods, *Phys Chem B* 108, pp.5882–5888.

[52]. Jian Zhu, Fan Zhang, Jian-Jun Li and Jun-Wu Zhao, (2014) The effect of nonhomogeneous silver coating on the plasmonic absorption of Au–Ag core–shell nanorod, *Gold Bull*, 47, pp.47–55.

[53]. N.R. Jana, L. Gearheart and C.J. Murphy, (2001) Wet Chemical Synthesis of High Aspect Ratio Cylindrical Gold Nanorods, *J. Phys. Chem. B*, 105, 4065-4067.

[54]. J. Pérez-Juste et al, (2004) Electric-Field-Directed Growth of Gold Nanorods in Aqueous Surfactant Solutions, *Adv. Funct. Mater*, 14, 571-579.

[55]. A. Akouibaa, A. Derouiche and H. Redouane, (2014) Numerical study of the effects of polymeric shell on plasmonic resonance of gold nanorods, *Inter. Jou. of Com. Mater. Sci. and Eng.*, 3 (4), pp.1450024(1-19).

[56]. P. V. Asharani , Y. Lianwu , Z. Gong and S. Valiyaveetti, (2011) Comparison of the Toxicity of Silver, Gold and Platinum Nanoparticles in Developing Zebrafish Embryos, *Nanotoxicology,* 5(1), pp.43-54.